

CHAPTER -3
MATERIALS AND METHODS

MATERIALS AND METHODS

The materials and methods used in the present study are described below:

3.1. Forest ecosystem of the study (Kaziranga National Park):

A flux tower was erected inside the Kaziranga National Park (KNP), Assam, India to quantify the CO₂, H₂O and energy fluxes over the semi evergreen forest of KNP. The Kaziranga National Park stands on the edge of the Eastern Himalaya and the mighty river Brahmaputra flows across the park along with other rivers Diphlu and Mora Dhansiri (fig 3.1). Due to the presence of above rivers the national park faces heavy flood events especially around the monsoon season, which makes a major impact on the ecosystem every year. As a result of deposition of silt, the soil quality of the park is fertile and alluvial. The park falls under the administrative area of Nagaon and Golaghat districts of the state of Assam. The Kaziranga National Park is recognized as the World Heritage Site by UNESCO due to its uniqueness in terms of wild life and biodiversity. The forest was also declared as a tiger reserve. The Kaziranga National Park covers a large area of 858.98 square kilometer and has been divided in to five ranges as Burhapahar range, Agaratoli range, Kohora range, Bagori range and Biswanath ghat range. The park is center of attraction to tourists as it is the home of great one horned rhinoceros. The diverse nature of the ecosystem of Kaziranga has made it a unique forest located at North eastern region.

Kaziranga national park is the combination of different forest types and biomass [1]. The forest types that comprise the whole Kaziranga National Park are Alluvial Inundated Grasslands, Alluvial Savanna Woodlands, Tropical Moist Mixed Deciduous Forests and Tropical Semi-Evergreen Forests. As per Köppen climate classification the climate of the national park can be categorized as humid sub-tropical climate. The park experiences an average total annual rainfall of 3750 mm and average annual temperature of 23°C [2].

3.2. Location of the flux tower inside the forest:

The geographical location of the tower is at 26° 34' 48"N latitude and 93°6' 28"E longitude (fig 3.1). The experimental site is located inside the Burhapahar range and the distance of the range office from Tezpur University is approximately 55 km. The areal

distance of the tower from the nearby vehicular traffic road is approximately 12 km. The tower can be reached from nearest Burhapahar range office by foot only during monsoon and post monsoon season due to heavy water logging inside the forest. Frequent appearance of wild animals like rhinos, wild buffalos, bunch of wild elephants, tigers and swamp deers in the road to the tower, made it a challenging job for the team of research workers. The dominant plant species located in and around the flux tower are listed in table 3.1. The tower is surrounded by the semi evergreen vegetation and far beyond the grasslands and water bodies are predominantly present. The terrain of the tower location is relatively flat.

3.3. Eddy Covariance method:

Eddy covariance method is the most important and efficient method used in micrometeorology to quantify the gas exchanges between biosphere and atmosphere. The inward or outward flux of any gas over the area under investigation can be explained and represented by the covariance between vertical wind velocity component and the concentration of gas under study.

In case of turbulent flow of any gas in the atmosphere, the basic equation of vertical flux of that gas can be expressed mathematically as:

$$Flux = \overline{\rho w s}$$

In the above equation

ρ is air density and it can be easily obtained from temperature, humidity and pressure with the help of the ideal gas law [3],

w is the vertical component of wind speed which is obtained from the sonic anemometer.

s is the dry mole fraction of the gas under study in air and it is recorded from the high frequency gas analyzer.

The right hand side of the above equation can be broken in to mean and deviations from the mean using the technique of Reynolds decomposition.

$$Flux = \overline{(\bar{\rho} + \rho')(\bar{w} + w')(\bar{s} + s')}$$

In the above equation prime symbol represents deviation from the mean.

After multiplication of the right hand side of the above equation the equation will become very large. After that, it is assumed that fluctuations of air density is zero and considering mean vertical flow to be negligible the above equation can be converted to the following equation:

$$Flux = \bar{\rho} \overline{w/s'}$$

Thus, eddy flux can be defined as the product between average density of air and the average covariance between deviations in vertical component of wind speed and the mixing ratio. Using the above equation flux of any gas (e.g. CO₂, CH₄) can be computed.

Sensible heat flux can be estimated by the product between the average air density and covariance between instantaneous deviations in vertical component of wind speed and the temperature:

$$H = \overline{\rho_{air}} C_p \overline{w/T'}$$

C_p is the specific heat of air at constant pressure.

Similarly, the latent heat flux can be estimated as;

$$\begin{aligned} LE &= \lambda \times \text{Water vapour flux} \\ &= \lambda \times \frac{m_w/m_{air}}{\bar{p}} \times \overline{\rho_{air} w/e'} \end{aligned}$$

Where, λ is constant, m_w is the molar mass of water, m_{air} is molar mass of air, ρ_{air} is dry air density and e is the water vapour mixing ratio.

Using high frequency measurement of three wind components and water vapour mixing ratio the evapotranspiration flux (ET) of any ecosystem can be computed as:

$$ET = \overline{\rho_{air}} \overline{w/e'}$$

Evapotranspiration flux is expressed in the units of mm hr⁻¹.

3.4. Instrumentation on the tower:

A 50 meter tall iron tower (photograph 3.1) was erected inside the forest during the year 2014 for continuous monitoring of CO₂, water vapour and energy fluxes between the semi evergreen forest ecosystem of KNP and the atmosphere. A 50 meter tall iron tower

was erected inside the forest by the collaborative efforts of Tezpur Central University located at Tezpur in the Northeastern state of Assam, India and Indian Institute of Tropical Meteorology, Pune. The transportation of tower materials to the site from the nearest range office, soil digging and erection work of the tower was done manually since machineries were not allowed to take inside the forest. This investigation was funded by the Ministry of Earth Sciences, Government of India as a part of Metflux India project. Various slow and fast response sensors were installed at different heights of the tower by the research workers with the help of the engineers of LI-COR, USA. The tower was instrumented with eddy covariance system, vertical profiles for CO₂ concentration measurement and different slow sensors for the measurement of meteorological and radiation parameters at different heights. All the sensors and accessories were powered with the help of solar charged batteries. Inside the forest there was no provision for electricity. Batteries (8 numbers) were installed inside a small chamber (photograph 3.3). The batteries were charged with the help of solar panels and solar charge controller. Solar electric fence lines were erected around the tower (photograph 3.4) to protect the tower and instruments from wild animals. Technical help were provided by scientists from IITM, Pune and Savitribai Phule Pune University for installation of the tower and the sensors (photograph 3.5).

3.4.1. Eddy covariance system:

3.4.1.1. 3-D sonic anemometer (Wind Master Pro, Gill Instruments, UK):

The sonic anemometer was installed at a height of 37 meter on the tower near LI-7200, the anemometer was placed away from the tower to avoid flow distortion (photograph 3.6 a). Sufficient care was taken to minimize the north offset of the anemometer during the installation process. It was connected as auxiliary input to the LI-7550 (analyzer interface unit). It provides precise, accurate and high frequency data of three wind components with help of ultrasonic technology. The wind data was stored as compressed file on LI-7550.

3.4.1.2. CO₂-H₂O enclosed path analyzer (LI-7200, LI-COR, USA):

LI-7200 measures the densities of CO₂ and water vapour in the air. This analyzer (LI-7200, LI-COR, USA) was installed at a height of 37 meter on the tower (photograph 3.6 b). The site and system setup related metadata like installation height, separation of the

inlet tube of LI-7200 in all the directions with respect to the center of the anemometer were recorded. It is a closed path infrared gas analyzer. The analyzer uses non-dispersive infrared spectroscopy for the measurement of the gas density. Initially, infrared signal passes through different optical filters and after that the signal passes through the closed sampling cell and finally it reaches the detector. While passing through the sampling cell of LI-7200, a portion of the infrared radiation gets absorbed by the CO₂ and water vapour present in the air sample. The densities of CO₂ and H₂O can be computed between the ratios of the absorbed radiation and a reference level. In parallel to the measurement of gas densities the analyzer also records the temperatures and pressure fluctuations at very high speed. Using these records both dry and wet mole fractions of CO₂ was computed with the help of the inbuilt algorithm.

3.4.1.3. Flow module (7200-101, LI-COR, USA):

The flow module was placed one meter below the anemometer and the analyzer. The flow module was connected to LI-7550 (analyzer interface unit). Its role is to maintain a constant flow of air in the system. We fixed the flowrate at 15 lpm by adjusting the motor speed.

3.4.1.4. Analyzer interface unit (LI-7550, LI-COR, USA):

LI-7550 acts as data logger and it was placed near the flow module. The metadata related to the site, LI-7200 and the sonic anemometer was entered in the embedded software by connecting the LI-7550 with the computer via an ethernet cable. The high frequency data from sonic anemometer and LI-7200 were logged as compressed (.ghg format) files inside the memory drive of this unit. The stored data was collected by connecting a computer to LI-7550 using an ethernet cable with the help of the connecting software (LI-7200/LI-7500A 7.3.0).

3.4.2. Biomet sensors and data logger:

3.4.2.1. Data logger (CR3000, Campbell Scientific, USA):

The CR3000 data logger (Campbell Scientific) was placed on the tower at a height of 3 meter. The CR3000 data logger records the electrical outputs of all the sensors connected to it. The data logger was programmed with help of the programming language CR basic. The program was sent to the data logger using ‘Loggernet 4.2.1’ software from

computer. The recorded output electrical signals from all the connected sensors were converted to the respective scientific units by the preprogrammed algorithm of the data logger. The output of the all the connected sensors (as 1 minute and 30 minute average) were stored in the memory of CR3000 in compressed format. The output can be downloaded and converted to ASCII format with the help of the software Loggernet 4.2.1 by connecting a computer to the data logger (CR3000).

3.4.2.2. Four component net radiometer (NR01, Hukseflux, Netherlands):

This sensor was installed at a height of 24 meter on the tower and levelled properly. Sufficient care was taken to avoid the shadow of the tower on the sensor surface. This sensor was installed on the tower for the measurement of four important component of radiation. It measures the incoming and reflected components of short wave and long wave radiations separately. This radiometer uses thermopile sensors inside. This sensor converts incoming and outgoing components of short wave and long wave radiation in to respective four small output voltages. The respective output signals for each component were stored in the data logger CR3000. The stored data of the radiation components were collected in ASCII format by connecting the data logger to the computer with the help of the software loggernet 4.2.1.

3.4.2.3. Multicomponent weather Sensor (WXT520, Vaisala Oyj, Finland):

Two numbers of the multicomponent weather sensors were installed one at 8 meter and the other at 37 meter height on the tower. This sensor gives wind speed, air temperature, relative humidity, rain fall amount etc. This sensor uses ultrasonic transducers for wind measurement. Inside WXT520 a piezo electrical sensor was used for measurement of rainfall. In WXT520, the relative humidity and air temperature were estimated with the help of a circuit containing a RC oscillator and two reference capacitors. The data of wind speed, air temperature, relative humidity and rainfall from both the sensors were stored in CR3000 as both one minute and 30 minutes files. The stored data of the above weather parameters were collected by connecting the data logger to the computer with the help of the software loggernet 4.2.1.

3.4.2.4. PAR sensor (SQ-100 & 300 series, Apogee instruments, USA):

This sensor was installed at 24 meter height on the tower near the net radiometer. The number of photons in the wave length range 400 nm to 700 nm is the main driver of

photosynthesis. This sensor measures number of photons in this wave length range. The photosynthesis photon flux is generally represented in the units of $\mu\text{mol m}^{-2} \text{sec}^{-1}$. The data of photosynthetically active radiation were also stored on the same data logger CR3000 as 1 minute and 30 minute average. The stored PAR data was collected in ASCII format by connecting the data logger to the computer with the help of the software loggernet 4.2.1. The PAR (photosynthetically active radiation) is expressed as $\mu\text{mol m}^{-2} \text{sec}^{-1}$.

3.4.2.5. Soil heat flux plate (HFP01SC-20, Hukseflux, Netherlands):

Two numbers of soil heat flux plates were properly installed at a depth of 5 cm below the ground without disturbing the natural structure of soil. The output of the heat flux sensor is a voltage signal which is proportional to the heat passing through it. The sensor has the function of self-calibration. The soil heat flux readings from both the sensors were stored on CR3000 data logger as 1 minute and 30 minute average and were collected by connecting a computer to the data logger using the software loggernet 4.2.1.

3.4.2.6. Soil temperature sensor (Model: Therm-SS, Make: ICT International, Australia):

Soil temperature sensors were installed at five different depths of soil. The five different levels were at surface, 5 cm, 15 cm, 25 cm and 40 cm. These sensors are basically resistors and their resistance varies with temperature. The output voltage signals from these sensors were directly converted to temperature readings with the help of the conversion formula which was preprogrammed in the data logger. The temperature readings from these sensors were stored on CR3000 data logger as 1 minute and 30 minute average and were collected by using a computer.

3.4.3. Vertical profile measurement of CO₂ concentration at different heights:

CO₂ concentration was measured at different heights using the combination of LI-8150 multiplexer and LI-8100 analyzer control unit. The gas analysis (with the help of infrared gas analyzer) and data communication was performed by the LI-8100 analyzer control unit and all the systems were interconnected through the LI-8150 multiplexer. In our study, profile inlets were installed at eight different heights viz., 2 m, 4 m, 6 m, 8 m, 12 m, 16 m, 20 m and at 37 m. The profile inlets on the tower were connected to the multiplexer with the help of long tubes. The data were stored inside a memory card of

LI-8100. The CO₂ concentration data at different levels were exported as half hourly mean text files using the software LI-8100 file viewer 3.1.1.

3.5. Processing of EC data:

During our period of study EC data were collected in computer in monthly basis with the help of Ethernet cable and the software LI-7200 (version 7.3.0). The raw data were processed with the following steps.

3.5.1. Primary processing of the raw data:

For the processing of the raw EC data the software Eddy-Pro (version 6.2.0, LI-COR, USA) was used. In our system all the raw input data were in *.ghg* format. The high frequency 10 HZ data were converted to half hourly average form using the express mode processing option available on Eddy-Pro 6.2.0. Along with the *ghg* files a metadata file was also logged on the memory with all the necessary informations of the site and sensor. We have chosen embedded metadata file for the data processing. All the necessary corrections and spike removal protocols were taken care off during the primary processing of the data. The offset occurred during the wind measurement by the sonic anemometer have been compensated with the help of angle of attack corrections for each components [4]. The measurement error occurred due to any tilt in the anemometer was compensated by using the double rotation method [5]. For detrending of the data series the block averaging method was used [6]. Any time lag between the signals from sonic anemometer and LI-7200 were optimised with the help of covariance maximization method [7]. As per Vickers and Mahrt [8], the raw data in the time series were screened using the statistical tests like spike count and removal [9], amplitude resolution, drop-outs, absolute limits, skewness and kurtosis. As we used closed path analyser, the air density fluctuations were compensated by using mole mixing ratios in calculation of covariances, thus the bias due to decoupling of CO₂ and H₂O molecules in the tubing system of LI-7200 was avoided [10]. Frequency response corrections were performed by using the analytic high pass filtering method following Moncrieff et al., [11]. For low pass filtering the software followed the similar algorithm as proposed by Moncrieff et al., [12]. The quality checking of the processed data were done by flagging the data as per carbo Europe protocol [13].

3.5.2. Secondary spike removal of CO₂ fluxes:

Although rigorous correction steps were taken during the primary processing of raw data, the processed output data were found to have some unrealistic spikes. These spikes were also removed before analysing the data. Those spikes occurred in the time series due to some non-stationary or temporary advection phenomenon [14]. We have used a two-stage statistical method similar to Thomas et al., [15] for detection and removal of spikes from the data set. At first the positive and negative flux values were separated into two groups. Then the standard deviation of the positive group and negative group were calculated separately. After that positive values which were greater than the twice of the standard deviation of all positive flux values were removed from the data set. Next, the negative flux values which were less than the twice of the standard deviation of all negative flux values were eliminated from the data set. For the fine tuning of the data set one more filtering step in each month has been applied. For each month of the year, average plus the standard deviation ($x + \bar{x}$) and average minus the standard deviation ($x - \bar{x}$) was calculated. In each month, half hourly flux values greater than ($x + \bar{x}$) and less than ($x - \bar{x}$) were deleted from the data set. Similar kind of spike removal method was also tested and applied by Papale et al., [16].

3.5.3. Removal of negative night-time CO₂ fluxes:

After the above filtering steps some negative flux values in the data set were observed during the night. Negative flux values during the night usually represent net CO₂ assimilation by the ecosystem, which is not acceptable in our ecosystem. Those fluxes were considered as advection events which occurred during the calm condition of the atmosphere. In our study, all the negative CO₂ flux values occurred at the time when the global solar radiation (R_g) was less than 20 W m⁻² (i.e. at night time) were deleted from the data set.

3.5.4. Friction velocity (u*) correction of CO₂ fluxes:

Eddy covariance system often underestimates the CO₂ fluxes during the condition when turbulence in the atmosphere is very low. At this state CO₂ released during respiration may be drained out laterally. Thus, infrared gas analyser (LI-7200) on top of the canopy might underestimate CO₂ flux during this time. To overcome this issue we removed and replaced the data of the period when the atmosphere was very calm. We used the online

tool of Max planck institute for Biogeochemistry available on the link [https:// www.bgc-jena.mpg.de/REddyproc/brew/REddy proc.rhtml](https://www.bgc-jena.mpg.de/REddyproc/brew/REddy_proc.rhtml) for u^* filtering. In the online tool, the u^* threshold has been estimated with the help of moving point test as done by Papale et al., [16]. In our data set the u^* threshold of 0.37 m s^{-1} was estimated by using the tool. All the CO_2 flux data of the period when u^* was less than 0.37 m s^{-1} were deleted from the data set.

3.5.5. Spike removal of latent and sensible heat fluxes:

Latent heat flux values less than -100 W m^{-2} and greater than 800 W m^{-2} were removed from the data set. Similarly, sensible heat fluxes greater than 500 W m^{-2} and less than -150 W m^{-2} were deleted before gap filling. Similar threshold values of latent heat and sensible heat flux were used by Thomas et al., [15] for removal of unrealistic data.

3.5.6. Gap filling of the data:

As a result of the above data removal processes 33 % of total data were removed. The removed data were then gap filled by the inbuilt algorithms of the above Max-planck tool ([https:// www.bgc-jena.mpg.de/REddyproc/brew/REddy proc.rhtml](https://www.bgc-jena.mpg.de/REddyproc/brew/REddy_proc.rhtml)). The algorithm used in this tool used the same method as used by Falge et al., [17]. Additionally, the covariation of fluxes with meteorological parameters and the temporal autocorrelation of fluxes were also considered in the algorithm of the tool similar to Reichstein et al., [18]. During our study period the gaps in CO_2 , H_2O and energy fluxes occurred only due to the data rejection in the above filtering steps and all the meteorological data at the same time were available. Therefore, the online gap filling tool of Max planck institute used particularly the look up table method to fill the gaps. In case of similar meteorological conditions window size of 7 days was used. If the meteorological condition differed within the first 7 days, the window size was increased up to 14 days. The tool also performed uncertainty analysis by creating artificial gaps and filling of those gaps using the above procedure. The estimated root mean square error (RMSE) of the gap filled CO_2 flux data was $2.73 \pm 0.27 \mu \text{ mol m}^{-2} \text{ s}^{-1}$. The estimated RMSE error of CO_2 flux is closer to the RMSE error estimates of Rodda et al., [14] where they reported RMSE error of computed CO_2 flux to be $1.81 \pm 0.24 \mu \text{ mol m}^{-2} \text{ s}^{-1}$.

3.6. Measurement of leaf area index (LAI):

Plant canopy analyzer (LI-2200, LiCor Inc., USA) was used for the measurement of the changes in the canopy architecture. We measured the LAI around the flux tower at biweekly interval. During LAI measurement, first a single above canopy reading was taken to measure the direct radiation followed by five below canopy readings from different randomly chosen directions in a radius of 500 meter around the tower for the measurement of canopy intercepted light, this whole process was repeated for two more times. Thus the computed LAI was the mean of three above canopy readings and fifteen below canopy readings. Fifteen below canopy readings were taken for improvement of the spatial average of LAI. By definition LAI is the ratio between the area of green leaf to the area of the ground surface i.e leaf area per unit ground area [19]. The foliage quantity of canopy can be estimated by the principle of light attenuation when incoming radiation passes through the canopy. Orientation of the foliage can be estimated by measuring the light attenuation at several zenith angles. During the operation of the device LI-2200, the attenuation of diffused incoming radiation at five different zenith angles gets recorded and stored. Thus for each above canopy measurement five readings gets stored, similarly five reading gets stored for below canopy measurement also. Thus the transmittance can easily be obtained for each zenith angle. Using this principle LI-2200 computes LAI.

3.7. Partitioning of net ecosystem exchange (NEE):

3.7.1. Calculations of NEE of CO₂:

We have calculated net ecosystem exchange of CO₂ by adding turbulent CO₂ flux above the canopy estimated by eddy covariance method to the storage CO₂ flux [20].

$$NEE = F_{ed} + S_r$$

F_{ed} is the turbulent CO₂ flux above the canopy and S_r is the storage flux.

Storage flux was estimated from the changes in half hourly CO₂ concentration at 37 meter height above the canopy using the EC sensor. We used only EC sensor concentration because measurement of CO₂ concentration at different levels using vertical profiles was not available during the period of our study.

$$S_r = \frac{P}{RT} \frac{\partial c(h)}{\partial t} h$$

Where, P denotes atmospheric pressure, T is air temperature, R is the molar gas constant, c denotes concentration of CO₂, h is the height where the concentration of CO₂ was recorded. $\partial c(h)$ was calculated from the difference of average CO₂ concentration between two half hourly intervals.

3.7.2. Partitioning of NEE in to gross primary production and ecosystem respiration:

Partitioning of net CO₂ flux in to component fluxes, gross primary production (GPP) and ecosystem respiration (Re) was done by using the online tool of Max planck institute ([https:// www.bgc-jena.mpg.de/REddyproc/brew/REddy proc.rhtml](https://www.bgc-jena.mpg.de/REddyproc/brew/REddyproc.rhtml)). We used day time based method for flux partitioning as discussed by Lassop et al., [21]. In the day time based algorithm of the partitioning tool, NEE was modeled by fitting a rectangular hyperbolic light response curve as per Falge et al., [17].

$$NEE = \frac{xyR}{xR + y} + r$$

In the above equation,

x is the canopy light utilization efficiency $\mu\text{mol C J}^{-1}$.

y is the maximum CO₂ uptake rate at light saturation condition $\mu\text{mol C m}^{-2} \text{ s}^{-1}$.

r is ecosystem respiration $\mu\text{mol C m}^{-2} \text{ s}^{-1}$

R is the incoming global solar radiation W m^{-2} .

The above rectangular hyperbolic light response function has been modified in to a different form which considers the temperature dependency of ecosystem respiration as discussed by Gilmanov et al., [22]. Therefore, in the algorithm, r of the above equation was substituted by the respiration model as discussed by Lloyd and Taylor [23].

$$NEE = \frac{xyR}{xR + y} + r \exp\left(E_0 \left(\frac{1}{T_{rf} - T_0} - \frac{1}{T_a - T_0} \right)\right)$$

The values of T_{rf} and T_0 was kept at 15 °C and -46.02 °C respectively similar to [18] in night time based flux partitioning tool.

The activation energy parameter E_0 was estimated from the night time data when $R < 4 \text{ W m}^{-2}$. In the next step, keeping E_0 as fix, the values of x , y and r were estimated using the data from day time.

In the algorithm followed by the online tool, care was taken to nullify the effect of VPD limitation on GPP following Korner et al., [24]. At higher VPD values, y of the above equation was replaced by:

$$y = y_0 \exp(-k(\text{VPD} - \text{VPD}_0)), \text{ VPD} > \text{VPD}_0,$$

$$y = y_0, \text{ VPD} < \text{VPD}_0$$

The parameter k was estimated using a data window of each four day which quantified maximum carbon uptake to GPP. The threshold VPD_0 was fixed at 10 hPa following Korner et al., [24].

3.8. Soil sample analysis:

Soil samples were collected from four different sites at four different directions of the tower during four different seasons of the year (i) winter (December to February) (ii) pre-monsoon (March to May) (iii) monsoon (June to September) and (iv) post monsoon (October to November). The four different sites were chosen randomly and kept fixed for the all the seasons. Soil samples were collected from two different depths (0-15 cm) and (15-30 cm). For sample collection we used a soil core sampler (60 cm length and 7 cm inner diameter). The collected samples from the forest were immediately stored inside the zipped plastic bags and were brought to the laboratory. The samples were then air dried for a period of 7 days. The dried soil samples were then sieved with the help of 2 mm sieve in the laboratory to remove all the residues from the soil.

3.8.1. Determination of soil organic carbon (SOC %):

The organic carbon content of the soil samples was determined with the help of dry combustion method [25] in Multi NC 2100S TOC analyzer, Analytic Zena, Germany. Inorganic carbon from the soil samples were removed by adding 10 % Hydrochloric acid to 0.05 gram of soil samples in combustion boat. The hydrochloric acid was added drop wise until the reaction completely stops. Most of the CO_2 gas emitted during the reaction were allowed to escape to the atmosphere immediately. After that the sample and acid were kept for a minimum time of 3 hours in a drying cup board at temperature of $105 \text{ }^\circ\text{C}$

until the excess moisture and hydrochloric acid gets evaporated. After that the organic carbon content of the soil samples were analyzed using the combustion furnace of the TOC analyzer.

3.8.2. Determination of soil organic carbon storage in soils:

The concentration of SOC in the soil samples was converted to mass by using the formula of Benbi et al., [26]:

$$SOC(Mg\ ha^{-1}) = C\% \times bulk\ density(Mg\ m^{-3}) \times depth(m) \times 100$$

Samples were collected during winter, pre-monsoon, monsoon and post monsoon seasons of the year 2016.

Amount of SOC sequestered by soil ($Mg\ C\ ha^{-1}$) during the period of study was calculated as:

$$= SOC\ at\ post\ monsoon\ season - SOC\ at\ winter\ season.$$

3.8.3. Soil p^H and conductivity:

10g of soil sample was mixed with 25 ml of water and a 1: 2.5 soil solution was prepared. After that the solution was stirred using a glass rod for half an hour. The pH of the prepared suspension was measured using a pH meter (model-H196107, made in Italy) and conductivity of the soil was measured using a conductivity meter (model-ULSTD61010A-1, made in Germany).

3.8.4. Bulk density of soil samples ($Mg\ m^{-3}$):

Bulk density of the soil samples were determined by the method of Kukal et al., [27]. Soil samples were collected using a hammer and an iron core from two different depths in the four seasons from the four sampling sites. The diameter of the used iron cores were 5 cm. The weight (W1) and volume (V) of the empty iron core was measured before the sampling process. The iron core was inserted in to the soil up to the respective depths in each time using a hammer. Using a sharp and thin knife the extra soil from upper and lower part of the tubes were removed. Next, the tubes with the soils were zipped locked in plastic bags and brought to laboratory. The cores with soil inside were kept at 105 °C inside an oven for a period of 48 hours until a constant weight (W2) was obtained. The bulk density was calculated using the following relation:

$$B.D = \frac{W2-W1}{V} Mg\ m^{-3}$$

3.8.5. Determination of porosity of soil (%):

Particle density of the soil was measured for estimating porosity. First the weight of a 100 ml empty bottle (W1) was taken, after that the bottle was completely filled with water and reweighed (W2). The water was then drained away from the bottle and it was dried. Then the bottle was partially filled with dry soil and the weight was taken (W3). The remaining empty portion of the bottle was completely filled with water and weight of this combination was taken (W4).

Particle density (P.D) was calculated as

$$= \frac{W3-W1}{W2+W3+W4-W1-W4}$$

The porosity was estimated using the values of B.D and P.D:

$$Porosity(\%) = \frac{P.D - B.D}{P.D} \times 100$$

3.8.6. Water holding capacity of soils (%):

The water holding capacity of the forest soil was estimated using the method given by [28]. An aluminum box was taken and a properly cut filter paper was placed inside the aluminum box. The weight of the filter paper plus the box was taken in an electronic balance. After that the box was completely filled with soil and care was taken to uniformly distribute the soil inside the box. Proper leveling of the upper surface of the box was done with the help of spatula. Then the weight of the combination was taken. The box plus soil was then placed on a petridish. Then the water was poured in to the petridish in such a way that one third of the box remained under the water. This set up was kept undisturbed for overnight. The box was then withdrawn from the water and properly wiped and the weight of the box was taken. A filter paper was given a shape similar to the base part of the box and the weight was taken. The filter paper was then emerged in to the water and immediately pulled back and then the weight was taken. The water absorbed by the filter paper was estimated by subtracting dry weight of the paper from the wet weight of the paper.

The following relation was used to determine the percentage of water content in soil:

$$Water\ holding\ capacity(\%) = \frac{W3 - W2 - W4}{W2 - W1} \times 100$$

Where,

W1= weight of (box + filter paper)

W2= weight of (box+ dry soil+ filter paper)

W3= weight of (box + filter paper+ wet soil)

W4=water absorbed by filter paper

3.8.7. Particle size analysis (sand, silt, clay %):

Particle size analysis was done by International Pipette Method as given by Page et al., [29] for particle size analysis:

The following reagents were used in the analysis: 6 % H₂O₂ (Hydrogen peroxide) and 2.5 % Sodium hexametaphosphate.

10 g of soil was taken in a beaker (500 ml) where 60 ml of 6% H₂O₂ was added and the mixer was kept overnight. In the next day again 30 ml H₂O₂ was poured and the mixer was boiled in a water bath and kept for overnight. On the next day, 15 ml of 2.5 % Sodium hexa meta phosphate was added to the content and the solution was stirred for 6 hours with the help of a mechanical shaker. On the proceeding day the content was transferred to a measuring cylinder of 1000 ml and the volume was topped up using distilled water. The proper mixing of the solution was done by rigorous shaking for about 1 minute. Then the solution was allowed to get stable. This time was taken as beginning time (t=0) and the room temperature was noted. Using the decantation chart the time needed for sedimentation of different soil particles was estimated.

3.8.7.1. Estimation of silt and clay fraction:

20 ml of the above content was pipetted out by dipping the pipette to 10 cm depth of the measuring cylinder. The content was then transferred into a pre-weighted porcelain basin following the time mentioned in the decantation chart. The basin was kept overnight in an oven at 105 °C. Next, the basin was brought out from the oven then cooled and weighted. Now using the following formula the percentage of clay and silt fractions was calculated:

Percentage of silt and clay

$$\begin{aligned} &= \frac{\text{weight of the sediment} \times 10^3 \times 10^2}{\text{volume of content taken(ml)} \times \text{weight of soil taken(g)}} \\ &= \text{weight of the sediment} \times 400 \end{aligned}$$

In the above relation,

$$\begin{aligned} \text{weight of the sediment} \\ &= \text{weight of the basin taken out from the oven} \\ &\quad - \text{initial weight of the basin} \end{aligned}$$

3.8.7.2. Estimation of clay fraction:

Again, 20 ml of the above content was pipetted out by dipping the pipette to 10 cm depth of the measuring cylinder. The content was then transferred into a pre-weighted porcelain basin following the time mentioned in the decantation chart. The basin was kept overnight in an oven at 105 °C. Next, the basin was brought out from the oven then cooled and weighted. Now using the following formula the percentage of clay was calculated:

$$\begin{aligned} \text{Percentage of clay} &= \frac{\text{weight of the sediment} \times 10^3 \times 10^2}{\text{volume of content taken(ml)} \times \text{weight of soil taken(g)}} \\ &= \text{weight of the sediment} \times 400 \end{aligned}$$

3.8.7.3. Estimation of silt fraction:

Percentage of silt fraction was calculated using the following relation:

$$\text{Percentage of silt} = \text{percentage of silt and clay} - \text{percentage of clay}$$

3.8.7.4. Estimation of sand fraction:

Percentage of sand fraction was calculated using the following relation:

$$\text{Percentage of sand} = 100 - (\text{percentage of silt and clay})$$

3.8.8. Determination of available nitrogen in soil (Kg ha^{-1}):

Available N in the soil was estimated by Kjeldhal distillation method [29]. 5 g soil sample was taken in a distillation flask to which 20 ml distilled water was added. After that this solution was mixed with 100 ml of 0.332 % KMnO_4 , 100 ml of 2.5 % NaOH solution and 2-3 drops of liquid paraffin was in a distillation flask. The organic matter present in the soil was oxidized using nascent oxygen which was released due to the presence of KMnO_4 in alkaline medium along with NaOH , ammonia was released during this process. The volume of distilled ammonia absorbed in a known volume of standard acid (20 ml 2 % boric acid) was taken in a conical flask. After the distillation, the resulted ammonia solution was titrated by using 0.02 N H_2SO_4 . Same treatments were applied with a soil free blank solution. The burette reading was corrected by subtraction of the blank solution reading from the earlier reading of the sample. Thus the consumed volume of acid (V) during titration was obtained. The available nitrogen was estimated by using the following formula:

$$\text{Available nitrogen in soil}(\text{Kg ha}^{-1}) = \frac{V \times 0.02 \times 0.014}{w \times 2.24 \times 10^6}$$

Where,

V is volume of 0.02 N H_2SO_4 consumed during titration

w is weight of soil sample

3.8.9. Determination of available phosphorous (Kg ha^{-1}):

The available phosphorous in the soil was estimated by using the method of Bray and Kurtz [30]. Initially 5 gram of soil was extracted by mixing 0.03 N NH_4F and 0.025 N HCL (50 ml) to remove the acid soluble P. The following reagents were used during the estimation of P (a) Bray and Kurtz number 1 extracting solution. This was prepared by dissolving 22.2 gram NH_4F and 41.6 ml concentrated HCL in distilled water and prepared the solution 0.03 M NH_4F in 0.025 M HCL (b) Reagent X, for this 12 gram of ammonium molybdate was mixed in 50 ml distilled water, next 0.2908 antimony potassium tartarate was mixed with 100 ml of water. The above two solutions were again mixed thoroughly with 1000 ml of 2.5 M H_2SO_4 and the volume was raised to 2000 ml (c) Reagent Y, to prepare this 1.056 gram ascorbic acid was mixed with 200 ml of prepared reagent X (d) 2.5 M H_2SO_4 (e) Standard stock P solution, this was prepared by dissolving 0.439 gram of KH_2PO_4 (potassium dihydrogen orthophosphate) in 500 ml

distilled water and 7N H₂SO₄ (25 ml) and the volume was raised to 1 liter, thus 100 ppm P standard stock solution was obtained, from this stock solution 2 ppm P solution was prepared by diluting it up to 50 times.

For the preparation of standard curves 1,2,3,4 and 5, 10 ml of 2 ppm P solution was taken in a volumetric flask of 25 ml and to this 5 ml extracted solution was added. The volume was raised up to 20 ml by adding distilled water and to this 4 ml of Y solution was added. After 10 minutes, the intensity of blue color was measured in a spectrophotometer at wavelength 882 nm [31]. 2.5 gram of dry soil sample and 25 ml of the extracted solution was mixed in an Erlenmeyer flask of 150 ml. Using a reciprocating shaker the suspension was shaken for 5 minutes. The solution was filtered using a Whatman number 42 filter paper. After that 5 ml aliquot of the extract was put inside a 25 ml volumetric flask and mixed with 20 ml distilled water and 4 ml of reagent Y. After waiting for 10 minutes the intensity of blue color was noted in a spectrophotometer at 882 nm.

The formula used to determine available P (in kg ha⁻¹) was

$$= A \times K1/w \times K2/K3 \times 2.24$$

Where,

A= concentration of P calculated from the standard curve

K1 = Volume of extractant

K2 = Volume after make up

K3= Volume of aliquot taken

w= Sample weight

3.8.10. Determination of available potassium (kg ha⁻¹):

Available potassium was analyzed with the help of Systronics flame photometer 128 (made in India) [29]. The following reagents used for estimation of available K

- (a) Neutral normal ammonium acetate (NH₄OAc): 77 gram of NH₄OAc was dissolved in distilled water and the volume was raised up to 1 liter.
- (b) Stock solution: 1.907 gram dried KCL at 110 °C was dissolved in 1000 mL deionised water and a strength of 1000 mgL⁻¹ was achieved.

To draw a calibration curve standards of 0, 5, 10, 15, 20, 25 and 30 ppm was prepared using 1000 ppm K and NH₄OAc. For analysis 10 gram of soil solution was taken inside a 250 ml conical flask. 100 ml of NH₄OAc (pH=7) solution was then added to the conical flask. After shaking the contents for half an hour, the solution was filtered through Whatman number 1 filter paper. The filtered product was analyzed using flame photometer at wavelength 767 nm.

Finally,

The available K in Kg ha⁻¹ was estimated using the relation

$$K = X \times V_{ex} / W_s \times 2.24$$

Where,

X is the concentration of K obtained from standard curve,

V_{ex} is volume of the extract

W_s is weight of the sample

3.8.11. Determination of C/N ratio of soil samples:

The total carbon and total nitrogen content of the sieved and air dried soil samples were estimated by CHN analyzer (model: 2400 series 2, PERKIN ELMER, USA). Percentages of total carbon and total nitrogen for each soil sample were recorded from CHN analyzer.

C/N ratio for each sample was estimated as:

$$\frac{C}{N} = \frac{\text{Percentage of total carbon in the sample}}{\text{percentage of total nitrogen in the sample}}$$

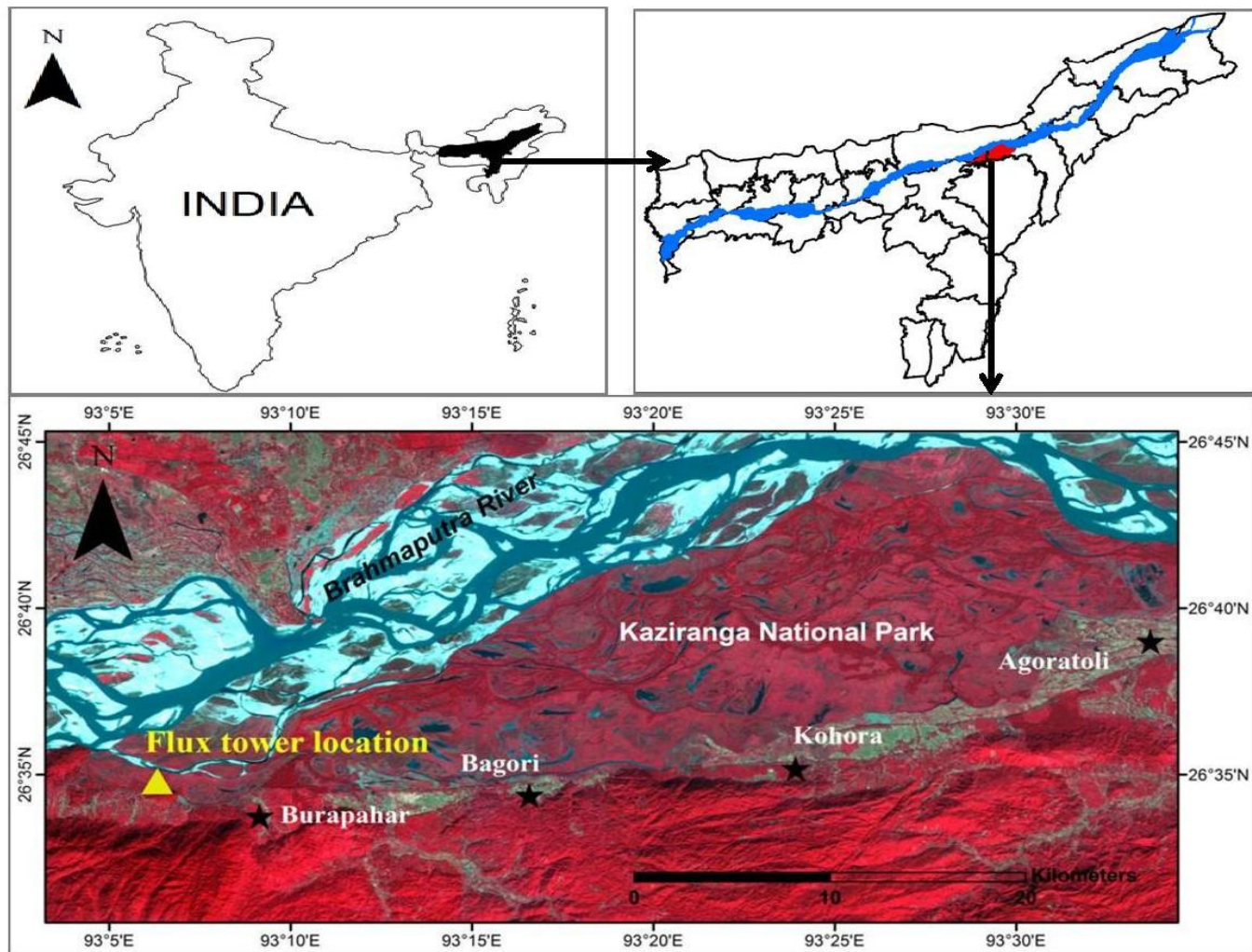


Fig 3.1: Location map of study area at KNP.

Table 3.1: List of dominant plant species around the tower.

Sl. No.	Scientific Name	Family	Canopy /height
1.	<i>Gmelina arborea</i> Roxb.	Lamiaceae	Medium
2.	<i>Mallotus repandus</i> (Willd.) Müll.Arg.	Euphorbiaceae	High
3.	<i>Tetrameles nudiflora</i> R. Br.	Tetramelaceae	High
4.	<i>Psidium guajava</i> L.	Myrtaceae	Small
5.	<i>Dalbergia sissoo</i> DC.	Papilionaceae	High
6.	<i>Lagerstroemia speciosa</i> (L.) Pers.	Lythraceae	High
7.	<i>Derris indica</i> (Lam.) Bennet	Papilionaceae	High
8.	<i>Syzygium cumini</i> (L.) Skeels	Myrtaceae	High
9.	<i>Dysoxylum mollissimum</i> Blume	Meliaceae	High
10.	<i>Albizia lebbek</i> (L.) Benth.	Mimosaceae	Moderate
11.	<i>Bridelia retusa</i> (L.) A.Juss.	Phyllanthaceae	Moderate
12.	<i>Erythrina indica</i> Lam.	Papilionaceae	Moderate
13.	<i>Pennisetum purpureum</i> Schumach.	Poaceae	Low
14.	<i>Chrysopogon zizanioides</i> (L.) Roberty	Poaceae	Low

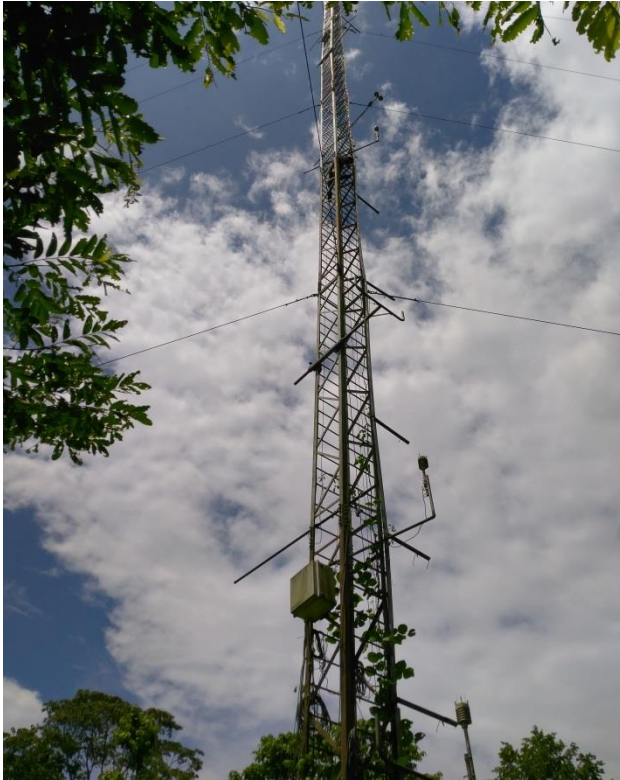


Photo 3.1: Photograph of the tower



Photo 3.2: Solar panels around the tower



Photo 3.3: Batteries inside the cabin



Photo 3.4: Electric fence around the tower



Photo 3.5: Installation of sensors on the tower during 2014



Photo 3.6: Eddy covariance system; (a) Sonic anemometer (b) LI-7200 closed path analyzer.



Photo 3.7: Road to the tower site during monsoon - a challenge.

References

- [1] Champion, H.G. and Seth, S.K. A revised survey of forest types of India; Government of India Press, New Delhi, 1968.
- [2] Heinen, J.T. and Shrivastava, R.J. An analysis of conservation attitudes and awareness around Kaziranga National Park, Assam, India: implications for conservation and development. *Population and Environment*, 30:261–274, 2009.
- [3] Burba, G., Madsen, R., and Feese, K. Eddy Covariance Method for CO₂ Emission Measurements in CCUS Applications: Principles, Instrumentation and Software. *Energy Procedia*, 40:329-336, 2013.
- [4] Nakai, T. and Shimoyama, K. Ultrasonic anemometer angle of attack errors under turbulent conditions. *Agricultural and Forest Meteorology*, 162-163:14-26, 2012.
- [5] Kaimal, J.C. and Finnigan, J.J. Atmospheric Boundary Layer Flows: Their Structure and Measurement. *Oxford university press*, 1994.
- [6] Pekour, M.S., Wesely, M.L., Martin, T.J., and Cook, D.R. A study of block averaging versus recursive filters for computing scalar eddy co-variances near the surface. In: American Meteorological Society 25th Conference on Agriculture and Forest Meteorology, Norfolk, VA, p144-45, 2002.
- [7] Langford, B., Acton, W., Ammann, C., Valach, A., and Nemitz, E. Eddy-covariance data with low signal to-noise ratio: time-lag determination, uncertainties and limit of detection. *Atmospheric Measurement Techniques*, 8(10):4197–4213, 2015.
- [8] Vickers, D. and Mahrt, L. Quality Control and Flux Sampling Problems for Tower and Aircraft Data. *Journal of Atmospheric and Oceanic Technology*, 14:512-526, 1997.
- [9] Mauder, M., Cuntz, M., Drue, C., Graf, A., Rebmann, C., Schmid, H.P., Schmidt, M., and Steinbrecher, R. A Strategy for Quality and Uncertainty Assessment of Long-term Eddy-covariance Measurements. *Agricultural and Forest Meteorology*, 169:122-135, 2013.
- [10] Ibrom, A., Dellwik, E., Larse, S. E., and Pilegaard, K. On the use of the Webb-Pearman-Leuning theory for closed-path eddy correlation measurements. *Tellus Series B-Chemical and Physical Meteorology*, 59:937-946, 2007.
- [11] Moncrieff, J. B., Clement, R., Finnigan, J., and Meyers, T. Averaging, detrending and filtering of eddy covariance time series, in Handbook of micrometeorology: a

- guide for surface flux measurements, eds. Lee, X., W. J. Massman and B. E. Law. Dordrecht: Kluwer Academic, 7-31, 2004.
- [12] Moncrieff, J. B., Massheder, J.M., De Bruin, H., Ebers, J., Friborg, T., Heusinkveld, B., Kabat, P., Scott, S., Soegaard, H., and Verhoef, A. A system to measure surface fluxes of momentum, sensible heat, water vapor and carbon dioxide. *Journal of Hydrology*, 188-189: 589-611, 1997.
- [13] Mauder, M. and Foken, T. Documentation and Instruction Manual of the Eddy Covariance Software Package TK2, *Arbeitsergebnisse*, Nr. 26, 2004.
- [14] Rodda, S.R., Thumaty, K.C., Jha, C.S., and Dadhwal, V.K. Seasonal Variations of Carbon Dioxide, Water Vapor and Energy Fluxes in Tropical Indian Mangroves. *Forests*, 7:35, 2016.
- [15] Thomas, M.V., Malhi, Y., Fenn, K.M., Fisher, J.B., Morecroft, M.D., Lloyd, C.R., Taylor, M.E., and McNeil, D.D. Carbon dioxide fluxes over an ancient broadleaved deciduous woodland in southern England. *Biogeosciences*, 8:1595-1613, 2011.
- [16] Papale, D., Reichstein, M., Aubinet, M., Canfora, E., Bernhofer, C., Kutsch, W., Longdoz, B., Rambal, S., Valentini, R., Vesala, T., and Yakir, D. Towards a standardized processing of Net Ecosystem Exchange measured with eddy covariance technique: algorithms and uncertainty estimation. *Biogeosciences*, 3:571–583, 2006.
- [17] Falge, E., Baldocchi, D., Olson, R., Anthoni, P., Aubinet, M., Bernhofer, C., Burba, G., Ceulemans, R., Clement, R., Dolman, H., Granier, A., Gross, P., Grunwald, T., Hollinger, D., Jensen, N.O., Katul, G., Keronen, P., Kowalski, A., Lai, C.T., Law, B. E., Meyers, T., Moncrieff, J., Moors, E., Munger, J.M., Pilegaard, K., Rannik, U., Rebmann, C., Suyker, A., Tenhunen, J., Tu, K., Verma, S., Vesala, T., Wilson, K., and Wofsy, S. Gap filling strategies for defensible annual sums of net ecosystem exchange. *Agricultural and Forest Meteorology*, 107:43–69, 2001.
- [18] Reichstein, M., Falge, E., Baldocchi, D., Papale, D., Aubinet, M., Berbigier, P., Bernhofer, C., Buchmann, N., Gilmanov, T., Granier, A., Grunwald, T., Havrankova, K., Ilvesniemi, H., Janous, D., Knohl, A., Laurila, T., Lohila, A., Loustau, D., Matteucci, G., Meyers, T., Miglietta, F., Ourcival, J.M., Pumpanen, J., Rambal, S., Rotenberg, E., Sanz, M., Tenhunen, J., Seufert, G., Vaccari, F.,

- Vesala, T., Yakir, D., and Valentini, R. On the separation of net ecosystem exchange into assimilation and ecosystem respiration: review and improved algorithm. *Global Change Biology*, 11:1424-1439, 2005.
- [19] Gonsamo, A. and Pellikka, P. Methodology comparison for slope correction in canopy leaf area index estimation using hemispherical photography. *Forest Ecology and Management*, 256:749-759, 2008.
- [20] Aubinet, M., Chermanne, B., Vandenhaute, M., Longdoz, B., Yernaux, M., and Laitat, E. Long term carbon dioxide exchange above a mixed forest in the Belgian Ardennes. *Agricultural and Forest Meteorology*, 108:293-315, 2001.
- [21] Lasslop, G., Reichstein, M., Papale, D., Richardson, A.D., Arneth, A., Barr, A., Stoy, P., and Wohlfahrt, G. Separation of net ecosystem exchange into assimilation and respiration using a light response curve approach: critical issues and global evaluation. *Global Change Biology*, 16:187-208, 2010.
- [22] Gilmanov, T.G., Johnson, D.A., and Saliendra, N.Z. Growing season CO₂ fluxes in a sagebrush-steppe ecosystem in Idaho: bowen ratio/energy balance measurements and modeling. *Basic and Applied Ecology*, 4, 167–183, 2003.
- [23] Lloyd, J. and Taylor, J.A. On the temperature dependence of soil respiration. *Functional Ecology*, 8(3):315-323, 1994.
- [24] Korner, C. Leaf diffusive conductances in the major vegetation types of the globe. In: Schulze, E.D. and Caldwell, M.M. (Eds.), *Ecophysiology of photosynthesis*. Springer, Berlin, 463–490, 1995.
- [25] Cihacek, L.J. and Jacobson, K.A. Effects of soil sample grinding intensity on carbon determination by high-temperature combustion. *Communications in Soil Science and Plant Analysis*, 38:1733-1739, 2007.
- [26] Benbi, D.K., Toor, A.S., and Kumar, S. Management of organic amendments in rice-wheat cropping system determines the pool where carbon is sequestered. *Plant and Soil*, 360(1-2):145-162, 2012.
- [27] Kukal, S.S., Rasool, R., and Benbi, D.K. Soil organic carbon sequestration in relation to organic and inorganic fertilization in rice-wheat and maize-wheat systems. *Soil and Tillage Research*, 102:87-92, 2009.
- [28] Chattopadhyaya, G.N. Chemical analysis of fish pond soil and water. Daya publishing House, New Delhi, India, 1998.
- [29] Page, A.L., Miller, R.H., and Keeney, D.R. Methods of soil analysis . Part 2,

Chemical and microbiological properties, 2nd ed., Agronomy No.9, ASA-SSSA, Madison, WI, USA, 1982.

- [30] Bray, R.H. and Kurtz L.T. Determination of total, organic and available forms of phosphorous in soils. *Soil Science*, 59:39-45, 1945.
- [31] Frank, K., Beegle, D., and Denning J. Phosphorus, in recommended chemical soil test procedures for the North Central Region, J.R. Brown eds., NC Regional Res. Publ. 221. Missouri Agric. Exp. Stn., Columbia, 21-26, 1998.